An assessment of pan-sharpening algorithm for mapping mangroves ecosystem: a hybrid approach

*Corresponding Author:

Naeem Shahzad

An assessment of pan-sharpening algorithm for mapping mangroves ecosystem: a hybrid approach

Naeem Shahzad [1, 2, *], Sajid Rashid Ahmad [2], Salman Ashraf [3]

[1]*Institute of Space Technology, 1-Islamabad highway, 44000, Islamabad, Pakistan*

[2]*Institute of Geology, University of the Punjab, Quaid e Azam Campus, Lahore, Pakistan*

[3]*GNS Science, 1 Fairway Drive, Avalon, Lower Hutt 5010, New Zealand*

ABSTARCT:

Mapping mangrove (littoral and swamps) ecosystems is challenging due to the qualitative and quantitative nature of the surrounding water and mudflats. However, accurate assessment of mangroves is required for to determine carbon credits. This research study explores five pan sharpening algorithms with the aim of determining the best algorithm to map mangrove ecosystems from very high resolution satellite images. In this research, a multidimensional evaluation was employed to pin point the best algorithm from among five advanced algorithms i.e. Ehler, Modified IHS, Wavelet, Optimized High Pass Filter Addition (OHPFA) and Subtractive Resolution Merge (SRM). These approaches involve the calculation of spectral RMSE, Sobel filter RMSE and correlation coefficient. OHPFA and SRM provided good results during this assessment. Object based image analysis was incorporated to further assess the best technique between these two approaches for assessing mangrove tree canopy by calculating under and over segmentation. The SRM algorithm provides the best results with a kappa value of 0.875 and an accuracy of 92.3% when compared with ground data. This research is very useful in various applications such as calculation of Crown Projection Area using high resolution satellite images for estimation of blue carbon in mangrove trees.

Keywords: Mangroves ecosystem, pan-sharpening algorithms, segmentation, blue carbon

1. Introduction

Tropical and subtropical coastal mangroves are among the most threatened and vulnerable

ecosystems worldwide (Valiela et al. 2001). They have an outstanding relevance ecologically and economically due to which there is an urgent demand for their conservation and restoration measures. Typical mangrove habitats are temporarily inundated and often located in inaccessible regions; consequently, traditional field observation and survey methods are extremely time-consuming and cost intensive. Remote sensing technology provides cost-effective tools to obtain detailed information for long term monitoring and mapping of highly threatened mangroves (Wang and Sousa 2009; Manson et al. 2001; Mumbay et al. 1999Green et al. 1998; Blasco et al. 2001; Giri et al. 2007; Everitt et al. 2008).

Advancements in technology have led to the development of various satellites (GeoEye 1, WorldView -2, and QuickBird etc.) that are designed to operate in two different modes; one to acquire high spatial resolution panchromatic images and other to acquire multispectral images with different spectral bands. For such earth observation data with very high resolution panchromatic (PAN) data, image fusion techniques referred to as 'pan-sharpening' are frequently used by remote sensing scientists in order to create a high resolution multi-spectral image (Blasco et al. 2001). A number of algorithms are available in different image processing software packages, for fusion of these images (Everitt et al. 2008). Details of these algorithms and techniques can be found in (Pohl and Van Genderen 1998; Garguet-Duport et al. 1996; Wenzhong et al. 2007; Ashraf et al. 2012; Ming and Li 2013; Ghosh and Joshi 2013). The most commonly used image fusion algorithms are the Brovey transformation (BT), Optimized high pass filter Addition (OHPFA), Principal component substitution (PCS), wavelet transformation (WT), Modified Intensity Hue Saturation (MIHS), multiplicative bilinear transformation (MBT), Ehlers fusion (EF), Gram-Schmidt (GS) sharpening and Subtractive resolution merge (SRM).

Previous studies have shown that the application of these fusion algorithms varies from preserving spectral content to highlighting the spatial details of objects (Blasco et al. 1998). Different evaluation techniques have been proposed and used by researchers to assess the best approach of pansharpening for various applications (Everitt et al. 2008) and to develop various metrics for the assessment. Most of these approaches are specifically designed such that they involve only pixel based analysis (Pohl and Van Genderen 1998; Hong-Gyoo et al. 2003; Santurri et al. 2010; Ashraf el at. 2012; Palubinskas 2013) and very few assessments have used Geographic object based image analysis (GEOBIA) (Jhonson et al. 2012 and 2013). GEOBIA is an emerging technique for image analysis and has been used in various applications (Blaschke et al. 2014). GEOBIA provides high level of accuracy particularly when dealing with very high spatial resolution multispectral images (Castilla 2003; Yan et al. 2006; Myint et al. 2008). In this, an input image is divided into different regions called "image segments" on the basis of criteria of homogeneity and heterogeneity, and then classified using various approaches generating a comprehensive and refined rule set (Shahzad et al. 2015; Johnshon et al. 2012). As, GEOBIA incorporates shape and size rather than Brightness Values (BV) of individual pixel, it will be an appropriate way of assessing the pansharpening quality even in the case of single tree canopy identification. Clinton et al. (2010) and Johnson et al. in (2012) discussed various approaches for evaluation of image segments generated using GEOBIA for different pansharpening approaches.

In this study, a multidimensional evaluation was employed to pin point the best fusion algorithm from among five advanced fusion algorithms i.e. Ehler, Modified IHS, Wavelet, Optimized High Pass Filter Addition (OHPFA) and Subtractive Resolution Merge (SRM). These algorithms were assessed to determine the best algorithm of pansharpening of very high resolution satellite images for mapping mangrove ecosystems and for various applications such

as biomass estimation in mangroves (referred to as ‘blue carbon’) as well as to clearly delineate the tree crown projection area (CPA), even for a single tree.

2. Materials and methods

Study Area

The Indus Delta of Pakistan is a typical fan-shaped delta, built up by the discharge of large quantities of silt washed down from upland and mountain areas. It covers an area of about 600,000 hectares and consists of more than 17 major creeks and innumerable minor creeks, mud flats and fringing mangroves (Meynell and Qureshi 1993).

The mangrove ecosystem (Figure 1) of this delta is unique in being the largest area of arid climate mangroves in the world. It consists of inter tidal fauna and flora found in the tropics and subtropics and is mostly covered by evergreen broad leaved trees with still roots or viviparous seedlings (UNESCO 1973).

The study area lies in the Keti Bander *taluka* of Thatta district of Sindh Province. It extends between 67°25'41.62"E, 24°14'47.87"N and 67°30'0.88"E, 24°12'30.24"N covering an area of 40 square kilometer from Tango creek to Kaddiaro creek as shown in Figure 1. This portion of forest consists of a variety of mangrove trees in terms of density of canopy cover along with the other land cover / land use classes. The major canopy cover classes present in the area are; dense mangroves (> 60% canopy cover), medium canopy mangroves (30%-60% canopy cover) and sparse mangroves (10%-29% canopy cover). The density covers of these three classes were defined on the basis of the Land Cover Classification System (LCCS) developed by the Food and Agriculture Organization (FAO) and the United Nations Environment Programme

(UNEP) (Di Gregorio 2005). The area has been selected in order to include all major vegetation types such as mangroves, *Prosopis* spp. marine algae, saltbushes and grasses for this ecosystem.

Data Acquisition

In this study, the images used were a sub scene of very high resolution satellite images i.e. WorldView-2. The extent of this sub scene is 3002 x 2027 pixels of multispectral and 12005 x 8105 pixels of panchromatic image (Figure 1) captured on 10th February 2010. These images were acquired from World Wide Fund for Nature (WWF) Pakistan. Both the acquired images of low resolution multispectral images (LRMI) (spatial resolution 1.85m at nadir) and high resolution panchromatic image (HRPI) (spatial resolution 0.46m) were in raw format and were geometrically projected to UTM zone 42N with WGS84 as a datum. The data characteristics of the acquired images can be found on Digital Globe data sheet (Digital Globe 2009).

Edge matching of Pan and multispectral images

Platforms such as QuickBird, Ikonos, GeoEye, WorldView-2 simultaneously collect panchromatic and multispectral images. Consequently, error in the precise alignments of the sensors causes a shift among the pixels of similar features in both the images.

However, the two images i.e. LRMI and HRPI should only be valuable for high resolution multispectral image (HRMI) if these have the features with same edges. To achieve this, the AutoSync tool of the image processing software (i.e. ERDAS Imagine) was used to co register the LRMI and HRPI (Knorn et al. 2009). Ground Control Points (GCPs) were selected and tie points were generated in order to get maximum control with root mean square error (RMSE) of not more than 0.1 pixels.

Image fusion

In this study, the candidate pansharpening algorithms were (1) Ehler, (2) Modified IHS (3) Wavelet transformation (4) Optimized High Pass Filter Addition (OHPFA) and (5) Subtractive Resolution Merge (SRM). These algorithms were applied to the WorldView image of study area using ERDAS Imagine 2013 and ENVI 5.1 softwares and qualitative assessment was done by visual inspection. The details of these candidate pansharpening methods can be found in a number of previous research papers (Wald et al. 1997, Ranchin and Wald 2000; Klonus and Ehlers 2007; Gangkofner et al. 2008; Witharana and Civco 2012; Ashraf et al. 2013) to understand the metrics and mathematical expressions. The major steps involved in this evaluation are shown in the evaluation workflow shown in Figure 2.

Ground truthing

In this study, a field campaign was carried out in collaboration with Wide Fund for Nature (WWF) to collect ground samples for Land cover (LC) mapping and accuracy assessment. In the field (Figure 3), access through the creeks was made by boats. *In situ* measurements were carried out to measure the canopy crowns of mangrove trees at different density levels i.e. closed, medium and open. The approach is discussed by Kauffman and Donato (2012) who used it to measure the canopy crowns of the mangroves. These measurements were used to assess the accuracies of various pansharpening algorithms during the segmentation process of GEOBIA. A stratified random sampling technique was used to collect 120 ground control points (GCPs) by using Garmin 76CSx global positioning system (GPS) device for various LC features e.g. closed and open canopy mangroves, salt bushes, algae, and water body, etc. Out of these 120 GCPs, 23 were used for mapping and remainder was used for accuracy assessment of the final outputs.

Delineation of reference polygons of the tree crown

High-resolution satellite image of WorldView-2 was used to delineate the boundaries of different canopies of mangrove trees on the basis of visual analysis and field survey measurements. These delineated polygons were used as a reference for the evaluation of the spatial accuracy of image segments for each pansharpening technique. Similar techniques were also used by Johnson et al. in 2012 and Tu et al. in 2012 (Johnson et al. 2012, Tu et al. 2012), but, in this study we have incorporated the field data in order to minimize the errors during the assessment process. Thirty-nine (39) reference polygons scattered throughout the area were delineated which comprised of mangroves of different crown canopy sizes (Figure 4).

Performance measure and quality assessment

The general requirements of an image fusion process are that it should preserve all valid and useful pattern information from the source images, while at the same time it should not introduce artifacts that could interfere with subsequent analyses. The performance measures adopted in this research provide some quantitative comparison among different schemes, mainly aiming at measuring correlation coefficient, spectral and spatial RMSE (Gangkofner et al. 2008) along with the over segmentation and under-segmentation by computing the D metrics (Clinton et al. 2010) which leads to the assessment of the most suitable techniques for the very high resolution satellite image for mapping the mangroves (Li et al. 2010; Wald et al. 1997).

Correlation Coefficient (CC):

Pearson's correlation coefficient is the most conventional similarity metric (Wang et al. 2005) to check the accuracy. While doing merging, the spatial gradient contained in the HRMI should resemble those under lying HRPI. The correlation coefficient between the HRMI and HRPI

illustrates the degree of similarity of their spatial gradients (Zhou et al. 1998). In this study 5 by 5 pixels' kernel was applied to both the HRPI and HRMI (Wang et al. 2005) to derive the CC.

Calculating the spectral Root Mean Squared Error (RMSE):

The Root Mean Squared Error (RMSE) measures the standard error between the LRMI and the HRMI (Gangkofner et al. 2008; Li et al. 2010). It quantifies the average amount of changes in brightness values (BV) due to the pansharpening and is a more sensitive criterion than Pearson's correlation. The RMSE can better distinguish the degree of similarity between MS and pansharpened data (Gangkofner et al. 2008). It can be categorized to calculate at a global and pixel level. It indicates that how close the BVs of MS and HRMI are with each other. The Equation (1) was used to calculate the RMSE (Pradhan et al. 2006) is;

$$\mathrm{RMSE_k} = \frac{\sum_{i,j=1}^{N} \sqrt{\left(B_k(i,j) - F_k(i,j)\right)^2}}{N^2} \quad (1)$$

Calculating the spatial Sobel filter based RMSE for spatial values of pixels:

The second spatial metric, i.e. Sobel filter based RMSE, is a quantitative approach for comparing the absolute edge magnitude difference of the HRPI and the fused HRMI and LRMI with HRMI as well. This filter based approach measures the gradient of edge intensities by using a kernel of 3×3 Sobel filters in the vertical and horizontal directions (Ashraf et al. 2012). The spectral distance of these two horizontal and vertical edge intensities produces an edge magnitude on the basis of the following Equations (2, 3 and 4) modified from Ashraf et al. 2012;

$$M = \sqrt{M_x^2 + M_y^2} \quad (2)$$

$$M_x = \begin{bmatrix} -1 & 0 & +1 \\ -2 & 0 & +2 \\ -1 & 0 & +1 \end{bmatrix} \times \mathrm{Image} \quad (3)$$

And;

$$M_y = \begin{bmatrix} -1 & -2 & -1 \\ -0 & 0 & 0 \\ +1 & +2 & +1 \end{bmatrix} \times \text{Image} \quad (4)$$

Image Segmentation and thematic layer generation:

Image segmentation was done in Definiens Developer 7®. A multiresolution segmentation approach was adopted due to its refined segments on the basis of homogeneity and heterogeneity (Shahzad et al. 2015) which has been used for many remote sensing studies (Benz et al. 2004). In the segmentation process, three user-defined parameters needs to be defined: a "Threshold" parameter that controls the relative size of segments, a "Shape" parameter that controls the relative amounts of spectral and spatial information used in the segmentation process, and a "Compactness" parameter that controls how smooth vs. how jagged segment boundaries are (Clinton et al. 2010). The most suitable scale parameter for each pansharpened layer was chosen using the Estimation of Scale Parameter (ESP) tool (Drăguţ et al. 2010) in order to minimize the human error for assessment.

Spatial accuracy of segments – calculation of over segmentation and under segmentation:

The D metric proposed by Clinton et al. 2010, provides a better performance than other metrics and has been used to calculate over and under segmentation. The term over segmentation refers to the segments which are smaller than the shape and size of the object of interest and can easily be understood from figure 5 (Witharana et al. 2013). . Mathematically it can be taken into account as Equation (5) (Clinton et al. 2010);

$$\text{OverSeg}_{ij} = 1 - (\text{area}(x_i \cap y_j)/\text{area}(x_i), y_j \in Y_i \quad (5)$$

Where area (xi, yj) is the area of the geographic intersection of reference polygon xi and image segment yj. Yi is the subset of segments relevant to reference polygon xi (i.e., segments for which either: the centroid of Xi is in the yj, the centroid of yj is in xi, where$(\frac{\text{area}(x_i \cap y_j)}{\text{area}(y_j)} > 0.5$, or

$(\mathrm{area}(x_i \cap y_j)/\mathrm{area}(x_i) > 0.5$, the values for the over-segmentation ranges from 0 to 1. Lower values represent less over-segmentation.

Under segmentation can be mathematically defined as Equation (6) (Clinton et al. 2010);

$$\mathrm{underSeg}_{ij} = 1 - (\mathrm{area}(x_i \cap y_j)/\mathrm{area}(y_j), y_j \in Y_i \quad (6)$$

These two segmentation parameters are combined to calculate D metrics explained in Equation (7);

$$D = \sqrt{\mathrm{OverSeg}_{ij}^2 + \mathrm{UnderSeg}_{ij}^2}\Big/2 \quad (7)$$

Higher spatial accuracy (i.e. less over and under segmentation) can be attributed to lower value of D and vice versa.

Spectral accuracy of segments – calculation of RMSE:

RMSE shown in equation (8) has been considered an effective approach for the assessment of homogenous and heterogeneous image regions (Li et al. 2010; Vijayaraj et al. 2006). The comparison of spectral characteristics of image objects/segments generated on the pansharpened satellite image with that of the segments generated on multispectral image made it easy to assess the spectral accuracy by calculating RMSE. In this study RMSE against each spectral band has been calculated in order to evaluate which band constitutes towards higher spectral accuracy. This was done by doing up sampling of original multispectral image to that of HRMI in order to make it comparable with the segments of panshapened image (Johnson et al. 2012).

$$\mathrm{RMSE} = \frac{\sqrt{\sum_{i=1}^{n}(\mathrm{pansharp}_i - \mathrm{multispectral}_i)^2}}{n} \quad (8)$$

Defining class hierarchy and applying classification schema:

In this study Geographic –object based image analysis (GEOBIA) was adopted after assessing the segments spatial and spectral accuracy (Hay and Castilla 2008). The classification process

was divided into the following steps: 1) importing the image, 2) applying the segmentation scheme, 3) defining hierarchy, 4) classification based on segmentation, 5) repeating the classification process for best results, and 6) final output (Laliberte et al. 2004).

Cognitive network language (CNL) provides a very useful interface to define class hierarchy to be used to classify image objects. It contains all the relevant classes in classification scheme under observation. Typical hierarchy used for this study is shown in Figure 6.

A rule set is basically set of algorithms that define or runs in process tree to assign classes to image object domain on the basis of defined algorithm (Blaschke 2014). A single rule/algorithm executes the image objects for one or more classes. A comprehensive rule set was developed and taken into account which was developed by incorporation of various useful parameters, like normalized difference vegetation index (NDVI) (Rouse et al. 1973), normalized difference soil index (NDSI) (Li and Chen 2014), normalized difference water index (NDWI) (Gao 1996) and soil adjusted vegetation index (SAVI) (Huete 1988).

Accuracy assessment

In this study, accuracy assessment of the classified pansharpened images were performed on the basis of ground control points collected during the field campaign. In total, 97 ground samples were collected to assess the accuracy of the output maps. The overall, user and producer accuracies were determined using a confusion matrix. Kappa value, standard error, and weighted error, with a 95% confidence interval for kappa were also calculated (Congalton 1996; Rosenfield and Fitzpatrick-Lins 1986).

3. Results and Discussion

Pansharpening results

Visual inspection technique is a subjective approach, which is used to assess and analyse the spatial (sharpness) and colour (spectral) quality of the image. Figure 7 shows a qualitative assessment of the pansharpening approaches i.e. Ehler's transformation, Modified IHS, wavelet transformation, OHPFA and SRM of the representative sub scene of original multispectral data. This visual comparison was added to bring an idea that how the output look like when compared visually (Zhang 2002). In this study the objective was not to highlight the approach that provides better visual results but rather to assess the best approach to minimal loss of original data values both spectrally and spatially. Visually in the figure 7 the subsets of ET (Figure 7b), WT (Figure 7d), OHPFA (Figure 7e) and SRM (fFgure 7f) seems to have similar outputs.

Spectral and spatial evaluation

The general requirements of an image pansharpening process are that it should preserve spectral and spatial information for the output data, while at the same time it should not introduce artefacts that could interfere with subsequent analyses. The performance measures adopted in this research provide some quality evaluation measures aimed at measuring the spectral root mean squareerror, correlation coefficient and Sobel filter assessment in order to assess the quality of the spatial component.

Table 1, elaborates the discrete values involved during the assessment of calculating spectral RMS, CC and Sobel filter RMSE at individual band level for each pansharpening approach. This assessment showed that, when doing spatial assessment, the least distortion in the spatial content of ET approach in for blue band and SRM provided better results for the other

bands. As this study focused on mangrove ecosystem, and keeping in view the vegetation content and its interaction with electro-magnetic radiations, SRM provided better results for NIR, and red bands (Table 1). On the other hand, CC and spectral RMSE showed quite different results highlighting OHPFA, SRM and ET in the queue for further assessment. OHPFA preserved spectral values for the blue band only (Table 1). ET and OHPFA showed maximum correlation for NIR and Red bands respectively leaving behind SRM for blue and green. OHPFA preserved the spectral value for the blue band when compared with SRM, which provided good results for the other bands (Table 1). The quality of OHPFA and SRM supports similar findings by Gangkofner et al. (2008) and Ashraf et al. (2012).

Figure 8 is a graphical representation of above discussion, plotted for the average values of correlation coefficient, spectral and spatial RMSE. It clearly shows that the modified IHS approach provided minimum correlation and highlights the second highest RMSE when compared with WT and ET. Considering the highest correlation and the minimum RMSE it can be deduced from Figure 8 that OHPFA and SRM provided relatively better results than the other techniques.

Spatial and Spectral Accuracy of Image Segments

In order to further assess the best approach for mapping mangroves ecosystem, these pansharpened images were assessed in Definien's environment, by generating and comparing the size and shapes of the segments with that of *in situ* ground data (Johnson et al. 2012). Figure 9 represents a sub-scene of segmented output image for each pansharpening technique. From this Figure 9, the analysis was done by comparing these shape and sized of the segments with the original *in situ* data of tree crown sizes. Multi-resolution segmentation approach has been adopted for the segmentation (Shahzad et al. 2015) and in order to minimize the human input and

to avoid trial and error methods of assigning parameters, ESP tool was used to automate the parameters.

D values for the most accurate segments calculated against each delineated tree crowns in the field for each pansharpening approach are shown in Table 2. From this Table 2, it is very clear that SRM provided lowest distortion (i.e. 0.7103) against delineated crown canopies of the mangroves trees. From the pixel based assessments, it was very hard to say that SRM provides better results because both OHPFA and SRM were quite close when considering CC and Sobel RMSE (Gangkofner et al. 2008; Ashraf et al. 2010) Hence, by incorporating the segmentation approach it showed that spatially SRM had less effect on the spatial accuracy of segmentation than the spatial information degradation of other approaches.

Spectral assessment was done by calculating the RMSE of each spectral band for every pansharpening approach (Table 3). This approach indicates that only two pansharpening methods are capable of producing segments with highest spectral accuracy i.e. lowest values when compared with the segments of original upsampled multispectral image. OHPFA provides good results in NIR band with value of 100.8 when compared with SRM which gives 101.7 error in NIR band but it provides highest possible accurate results in blue, green red than other techniques. Lower the value of RMSE, lower will be the error.

From Table 2 and Table 3, it is clear that all of the pansharpened images tended to produce more spatially-and spectrally accurate segmentations than the original PAN image and up sampled multispectral images respectively. High accuracy of SRM (Table 2) and OHPFA (Table 3) in NIR band were further evaluated by generating thematic layers and performing accuracy assessment.

Thematic layer generation

As object based image analysis provides high control to the pansharpened and high resolution data sets, so a comprehensive rule set was developed in order to generate thematic layers for all the output images (Figure 10).

The results of thematic layers strongly depends the quality of segments (Shahzad et al. 2015). The basic aim of thematic layer was to do accuracy assessments of the output results with that of field observation points. However, an overview of the output thematic layers generated using the defined and controlled rule set is shown in the figure 10.

Accuracy assessment of LCs

The accuracy assessments were done on the basis of GCPs collected during the field campaign. These samples comprised the field observation points against each defined class hierarchy (Figure 6). Table 4 shows an overall comparison of the classification accuracy and kappa values of each thematic layer of pansharpened outputs. The overall contribution of each class against each output image is summarized in the Table 4. From this table it can be seen that the highest accuracy of 92.3 and kappa value of 0.875 was attained by SRM technique when compared with accuracy of other techniques.

4. Conclusion

Mangroves ecosystem mapping requires the selection of suitable sensor which is capable of capturing the discrete information coming from the various features of the ground in the form of brightness values for the heterogeneous vegetation cover surrounded by water bodies. For this purpose, use of high quality data is more important for information extraction and analysis. In this study five advance pansharpening methods i.e. Ehler Transformation, Modified IHS, Wavelet Transformation, Optimized High Pass filter Addition (OHPFA) and Subtractive

Resolution Merge (SRM) were evaluated for mapping mangroves ecosystem. Qualitative and quantitative analysis were done to assess the most suitable technique.

Overall, SRM technique provided best results in this study keeping OHPFA at second. In the pixel based assessment (Table 1, Figures 7 and 8) OHPFA and SRM provided nearly accurate results when spectral RMSE, Sobel filter RMSE and CC were considered. This ambiguity and confusion was then analyzed through OBIA to check the loss of spectral and spatial content within the segments of homogeneous and heterogeneous pixels. This approach (Table 2 and Table 3, Figure 9) showed variety of different results keeping SRM at the highest level. The accuracy assessments of the generated land covers from each pan-sharpened image further highlighted the high quality of SRM. Gangkofner et al. in 2008 found that OHPFA gives the better results and at that time this technique was considered a modern technique for high resolution satellite data sets but in this study SRM takes lead in distinguishing objects more precisely than OHPFA. Similar results of proposing SRM for freshwater ecosystems were found by Ashraf et al. (2013).

In the light of GEOBIA framework, this hybrid approach found SRM to be the most suitable technique for mapping and assessing the mangroves ecosystem. OHPFA was found to be the second best pansharpening approach out of the various studied techniques. The outcomes of this study will be very helpful for various applications among which the accurate calculation of Crown Projection Area (CPA) using high resolution satellite data is particularly helpful in estimating the Blue carbon in this ecosystem,

5. Acknowledgements

The authors would like to thank the World Wide Fund for Nature (WWF) Pakistan for providing satellite data and field support. Without the field survey it would have been very hard to get into

the details regarding the measurements and GCP collection.

6. References

Ashraf, S., L. Brabyn, and B.J. Hicks. 2012. “Image data fusion for the remote sensing of freshwater environments.” *Applied Geography* 32(2): 619-628.

Ashraf, S., L. Brabyn, and B.J. Hicks. 2013. “Introducing contrast and luminance normalisation to improve the quality of subtractive resolution merge technique.” *International Journal of Image and Data Fusion* 4(3): 230-251.

Benz, U.C., P. Hofmann, G. Willhauck, I. Lingenfelder, and M. Heynen. 2004. “Multi-resolution, object-oriented fuzzy analysis of remote sensing data for GIS-ready information.” *ISPRS Journal of photogrammetry and remote sensing* 58(3): 239-258.

Blaschke T., G.J. Hay, M. Kelly, S. Lang, P. Hofmann, E. Addink, R. Queiroz Feitosa, F. Van der Meer, H. van der Werff, F. van Coillie, and D. Tiede. 2014. “Geographic object-based image analysis – towards a new parad*igm.” ISPRS Journal of Photogrammetry and Remote Sensing* 87: 180–191.

Blasco, F., M. Aizpuru, and C. Gers. 2001. “Depletion of the mangroves of Continental Asia.” *Wetlands Ecology and Management* 9(3): 255-266.

Blasco, F., T. Gauquelin, M. Rasolofoharinoro, J. Denis, M. Aizpuru, and V. Caldairou, V. 1998. “Recent advances in mangrove studies using remote sensing data.” *Marine and Freshwater Research* 49(4): 287-296.

Castilla, Guillermo. 2003. “Object-oriented analysis of Remote Sensing images for land cover mapping: conceptual foundations and a segmentation method to derive a baseline partition for classification. PhD. diss., Polytechnic University of Madrid

Clinton, N., A. Holt, J. Scarborough, L. Yan, and P. Gong. 2010. “Accuracy assessment measure for object-based image segmentation goodness.” *Photogrammetric Engineering & Remote Sensing* 76, 289–299.

Congalton, R.G. 1996. “Accuracy assessment: a critical component of land cover mapping.” in Gap analysis: a landscape approach to biodiversity planning, edited by J. M. Scott, T. H. Tear and F. Davis (Bethesda, Maryland: American Society for Photogrammetry and Remote Sensing). pp. 119–131.

Di Gregorio, A. 2005. “Land cover classification system: classification concepts and user manual” Environmental and natural resource series 8. Food & Agriculture Organization Rome, Italy. Available at: http://www.fao.org/docrep/008/y7220e/y7220e00.htm

DigitalGlobe. 2009. “World View 2 data sheet.” Available at: http://global.digitalglobe.com/sites/default/files/DG_WorldView2_DS_PROD.pdf

Drăguţ, L., D. Tiede, and S.R. Levick. 2010. “ESP: a tool to estimate scale parameter for multiresolution image segmentation of remotely sensed data.” *International Journal of Geographical Information Science* 24(6): 859-871.

Everitt, J.H., C. Yang, S. Sriharan, and F.W. Judd. 2008. “Using high resolution satellite imagery to map black mangrove on the Texas Gulf Coast.” *Journal of Coastal Research* 24(6): 1582-1586.

Gangkofner, U.G., P.S. Pradhan, and D.W. Holcomb. 2008. “Optimizing the high-pass filter addition technique for image fusion” *Photogrammetric Engineering & Remote Sensing* 74(9): 1107-1118.

Gao, B.C. 1996. “NDWI—A normalized difference water index for remote sensing of vegetation liquid water from space. *Remote sensing of environment* 58(3): 257-266.

Garguet-Duport, B., J. Girel, J.M. Chassery, and G. Pautou. 1996. “The Use of Multiresolution Analysis and Wavelets Transform for Merging SPOT Panchromatic and Multispectral Image Data.” *Photogrammetric Engineering & Remote Sensing.* 62(9): 1057-1068.

Ghosh, A. and P. Joshi. 2013. Assessment of pan-sharpened very high-resolution WorldView-2 images. *International Journal of Remote Sensing*, 34, 8336–8359.

Giri, C., B. Pengra, Z. Zhu, A. Singh, and L.L. Tieszen. 2007. “Monitoring mangrove forest dynamics of the Sundarbans in Bangladesh and India using multi-temporal satellite data from 1973 to 2000.” *Estuarine, Coastal and Shelf Science* 73(1): 91-100.

Green, E.P., P.J. Mumby, A.J. Edwards, C.D. Clark, and A.C. Ellis. 1998. “The assessment of mangrove areas using high resolution multispectral airborne imagery.” *Journal of Coastal Research* 14: 433-443.

Hay, G.J. and G. Castilla. 2008. “Geographic Object-Based Image Analysis (GEOBIA): A new name for a new discipline.” In *Object-based image analysis, edited by* Thomas Blaschke, Stefan Lang, Geoffrey J. Hay, 75-89. Springer: Berlin Heidelberg.

Hong-Goyoo S., Y. Konghyun, and C. Hoon. 2003. “Analysis of image fusion methods using IKONOS imagery.” *KSCE Journal of civil Engineering*. 7 (5): 577-584

Huete, A.R. 1988. “A soil-adjusted vegetation index (SAVI).” *Remote sensing of environment* 25(3): 295-309.

Johnson, B.A., R. Tateishi, and N.T. Hoan. 2012. “Satellite image pansharpening using a hybrid approach for object-based image analysis.” *ISPRS International Journal of Geo-Information* 1(3): 228-241.

Johnson, B.A., R. Tateishi, N.T. Hoan. 2013. “A hybrid pansharpening approach and multiscale object-based image analysis for mapping diseased pine and oak trees.” *International Journal of Remote Sensing* 34: 6969–6982

Kauffman, J.B. and D. Donato. 2012. “Protocols for the measurement, monitoring and reporting of structure, biomass and carbon stocks in mangrove forests” (No. CIFOR Working Paper no. 86, p. 40p). Center for International Forestry Research (CIFOR), Bogor, Indonesia.

Klonus, S. and M. Ehlers. 2007. “Image fusion using the Ehlers spectral characteristics preservation algorithm.” *GIScience & Remote Sensing* 44(2): 93-116.

Knorn, J., A. Rabe, V.C. Radeloff, T. Kuemmerle, J. Kozak, and P. Hostert. 2009. “Land cover mapping of large areas using chain classification of neighboring Landsat satellite images.” *Remote Sensing of Environment* 113(5): 957-964.

Laliberte, A.S., A. Rango, K.M. Havstad, J.F. Paris, R.F. Beck, R. McNeely, and A.L. Gonzalez. 2004. “Object-oriented image analysis for mapping shrub encroachment from 1937 to 2003 in southern New Mexico.” *Remote Sensing of Environment* 93(1): 198-210.

Li, S. and X. Chen. 2014. “A new bare-soil index for rapid mapping developing areas using LANDSAT 8 data.” *The International Archives of Photogrammetry, Remote Sensing and Spatial Information Sciences* 40(4): 139.

Li, S., Z. Li, and J. Gong. 2010. “Multivariate statistical analysis of measures for assessing the quality of image fusion.” *International Journal of Image and Data Fusion* 1(1): 47-66.

Manson, F.J., N.R. Loneragan, I.M. McLeod, and R.A. Kenyon. 2001. “Assessing techniques for estimating the extent of mangroves: topographic maps, aerial photographs and Landsat TM images.” *Marine and Freshwater Research* 52(5): 787-792.

Meynell, P. and T. Qureshi. 1993. “Sustainable management of mangroves in the Indus Delta, Pakistan.” in *Towards the Wise Use of Wetlands,* David, T. (ed.), 113-122, Ramsar Convention Bureau: Gland

Ming Liu and Li Shuhui. 2013. “An improved Image fusion algorithm based on his and wavelet transform.” *Applied mechanics and materials* 427-249: 1641-1644.

Mumby, P.J., E.P. Green, A.J. Edwards, and C.D. Clark. 1999. “The cost-effectiveness of remote sensing for tropical coastal resources assessment and management.” *Journal of Environmental Management* 55(3): 157-166.

Myint, S.W., M. Yuan, C.P. Cerveny, and R.S. Giri. 2008. “Comparison of remote sensing image processing techniques to identify tornado damage areas from landsat TM data.’ *Sensors* 8 (2): 1128–1156

Palubinskas, G. 2013. “Fast, simple, and good pan-sharpening method.” *Journal of Applied Remote Sensing* 7(1): 1-12

Pohl, C. and Van Genderen, J.L. 1998. “Multisensor image fusion in remote sensing: concepts, methods and applications.” *International Journal of Remote Sensing* 19: 823-854

Pradhan, P.S., R.L. King, N.H. Younan, and D.W. Holcomb. 2006. “Estimation of the number of decomposition levels for a wavelet-based multiresolution multisensor image fusion.” *Geoscience and Remote Sensing, IEEE Transactions on* 44(12); 3674-3686.

Ranchin, T., and L. Wald. 2000. “Fusion of high spatial and spectral resolution images: the ARSIS concept and its implementation.” *Photogrammetric Engineering and Remote Sensing* 66(1): 49-61.

Riyahi, R., C. Kleinn, and H. Fuchs. 2009. “Comparison of different image fusion techniques for individual tree crown identification using QuickBird images.” *International Society for Photogrammetry and Remote Sensing, High-Resolution Earth Imaging for Geospatial Information* 38: 1-4

Rosenfield, G.H., and K. Fitzpatrick-Lins. 1986. ‘A coefficient of agreement as a measure of thematic classification accuracy.” *Photogrammetric engineering and remote sensing* 52(2): 223-227.

Rouse Jr, J.W. 1972. “Monitoring the vernal advancement and retrogradation (green wave effect) of natural vegetation.” in *Prog. Rep. RSC 1978-1*, Remote Sensing Center, Texas A&M Univ., College Station, nr. (NTIS No. E73- 106393)

Myint, S.W., M. Yuan, C.P. Cerveny, R.S. Giri. 2008. “Comparison of remote sensing image processing techniques to identify tornado damage areas from landsat TM data.” *Sensors* 8 (2): 1128–1156

Santurri, L., R. Carlà, F. Fiorucci, B. Aiazzi, S. Baronti, M. Cardinali, and A. Mondini. 2010. “Assessment of very high resolution satellite data fusion techniques for landslide recognition.” In *ISPRS TC VII Symposium – 100 years ISPRS*. Wagner W., Székely, B. (eds.), XXXVIII (7B): 492-496. IAPRS: Vienna.

Shahzad, N., U. Saeed, H. Gilani, S.R. Ahmad, I. Ashraf, and S.M. Irteza. 2015. “Evaluation of state and community/private forests in Punjab, Pakistan using geospatial data and related techniques.” *Forest Ecosystems* 2(1): 1-13

Tu, T.M., C.L. Hsu, P.Y. Tu, and C.H. Lee. 2012. “An adjustable pan-sharpening approach for IKONOS/QuickBird/GeoEye-1/WorldView-2 imagery.” *Selected Topics in Applied Earth Observations and Remote Sensing, IEEE Journal* 5(1): 125-134.

UNESCO. 1973. *International Classification and Mapping of Vegetation*. United Nations educational, scientific and cultural organization: Paris

Valiela, I., J.L. Bowen, and J.K. York. 2001. “Mangrove Forests: One of the World's Threatened Major Tropical Environments.” *Bioscience* 51(10): 807-815.

Vijayaraj, V., N.H. Younan, and C.G. O’Hara. 2006. “Quantitative analysis of pansharpened images.” *Optical Engineering* 45(4): 046202-046202.

Wald, L., T. Ranchin, and M. Mangolini. 1997. ‘Fusion of satellite images of different spatial resolutions: assessing the quality of resulting images.” *Photogrammetric engineering and remote sensing* 63(6): 691-699.

Wang, L.E. and W.P. Sousa. 2009. “Distinguishing mangrove species with laboratory measurements of hyperspectral leaf reflectance.” *International Journal of Remote Sensing* 30(5): 1267-1281.

Wang, Z., D. Ziou, C. Armenakis, D. Li, and Q. Li. 2005. “A comparative analysis of image fusion methods.” *Geoscience and Remote Sensing, IEEE Transactions on* 43(6): 1391-1402.

Wenzhong, S.C., and Z. Shulong. 2007. “Fusing Ikonos Images by a Four-band Wavelet Transformation Method.’ *Photogrammetric Engineering and Remote Sensing* 73(11): 1285-1292.

Witharana, C. and D.L. Civco. 2012. “Evaluating remote sensing image fusion algorithms for use in humanitarian crisis management.” In proc. *SPIE 8538, Earth Resources and Environmental Remote Sensing/GIS Applications III*, 853807-853807. Edinburgh, United Kingdom.

Witharana, C., D.L. Civco, and T.H. Meyer. 2013. “Evaluation of pansharpening algorithms in support of earth observation based rapid-mapping workflows.” *Applied Geography* 37: 63-87.

Yan. G., J.F. Mas, B.H.P. Maathuis, Z. Xiangmin, P.M. Van Dijk. 2006. “Comparison of pixel-based and object-oriented image classification approaches — A case study in a coal fire area, Wuda, Inner Mongolia, China.” *International Journal of Remote Sensing* 27(18): 4039–4055.

Zhang, Y. 2002. “Problems in the fusion of commercial high-resolution satelitte as well as Landsat 7 Images and Initial Solutions.” *International Archives of Photogrammetry Remote Sensing and Spatial Information Sciences* 34(4): 587-592.

Zhou, J., D.L. Civco, D.L. and J.A. Silander. 1998. “A wavelet transform method to merge Landsat TM and SPOT panchromatic data.” *International Journal of Remote Sensing* 19(4): 743-757.

List of Tables

Table 1: Evaluation metrics for each individual spectral band

Data Fusion Technique	Spectral measure between LRMI and HRMI								Spatial measures between HRPI and HRMI			
	Correlation Coefficient				Spectral RMSE				Sobel Filter RMSE			
	Blue	**Green**	**Red**	**NIR**	**Blue**	**Green**	**Red**	**NIR**	**Blue**	**Green**	**Red**	**NIR**
ET	0.91	0.96	0.96	**0.91**	5.17	11.12	8.52	18.8	**109**	119.8	120	167.3
Modified IHS	0.81	0.893	0.94	0.85	4.18	13.41	10.2	37.8	111	99.42	155	165.8
WT	0.97	0.912	0.97	0.95	4.51	9.56	7.98	48.4	127	106.7	113	211.7
OHPFA	0.96	0.981	**0.99**	0.96	**3.39**	9.52	11.3	23.3	111	76.59	75.9	202
SRM	**0.97**	**0.983**	0.98	0.98	4.17	**2.13**	**6.78**	**17.1**	111	**69.68**	**67**	**127.3**

Table 2: D metric values (D) against parameters automated by ESP tool

Pansharpening Method (Mangrove trees)	D	Threshold	Shape	Compactness
ET	0.7319	15	0.3	0.6
Modified IHS	0.7652	10	0.4	0.5
OHPFA	0.7209	15	0.7	0.2
WT	0.7571	10	0.5	0.7
SRM	0.7103	10	0.6	0.3

Table 3: RMSE for each pan-sharpening method against each spatially accurate band

Pansharpening Method	Blue RMSE	Green RMSE	Red RMSE	NIR RMSE
ET	115.8	115.8	115.8	115.8
Modified IHS	136.8	102.6	85.5	179.2
OHPFA	102.5	81.1	74.3	100.8
WT	107.9	90.5	80.3	125.2
SRM	98.5	86.4	50.3	101.7

Table 4: Summarized results of accuracy tests for each pan-sharpened image

Accuracy type	LRMI	ET HRMI	Modified IHS HRMI	WT HRMI	OHPFA HRMI	SRM HRMI

Overall accuracy	**classification**	75	79	81	87	91	92.3
Overall kappa		0.638	0.641	0.735	0.832	0.798	0.8751

Figures

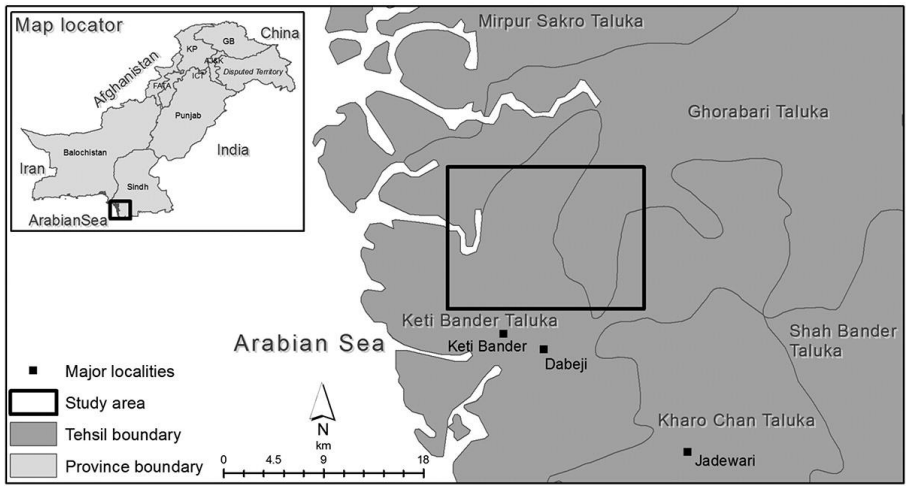

Figure 1. Location map of study area

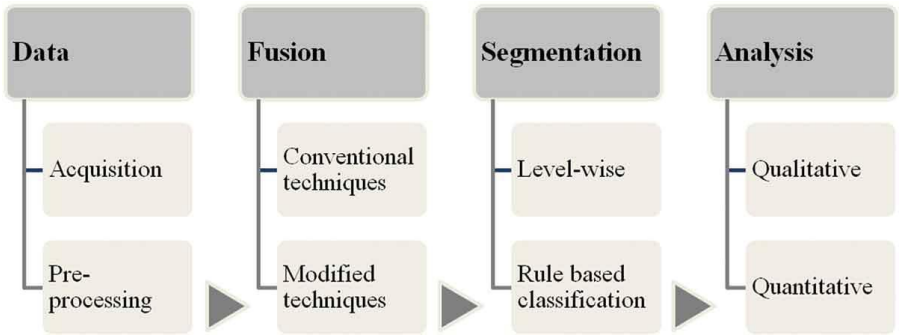

Figure 2. Workflow of the research approach

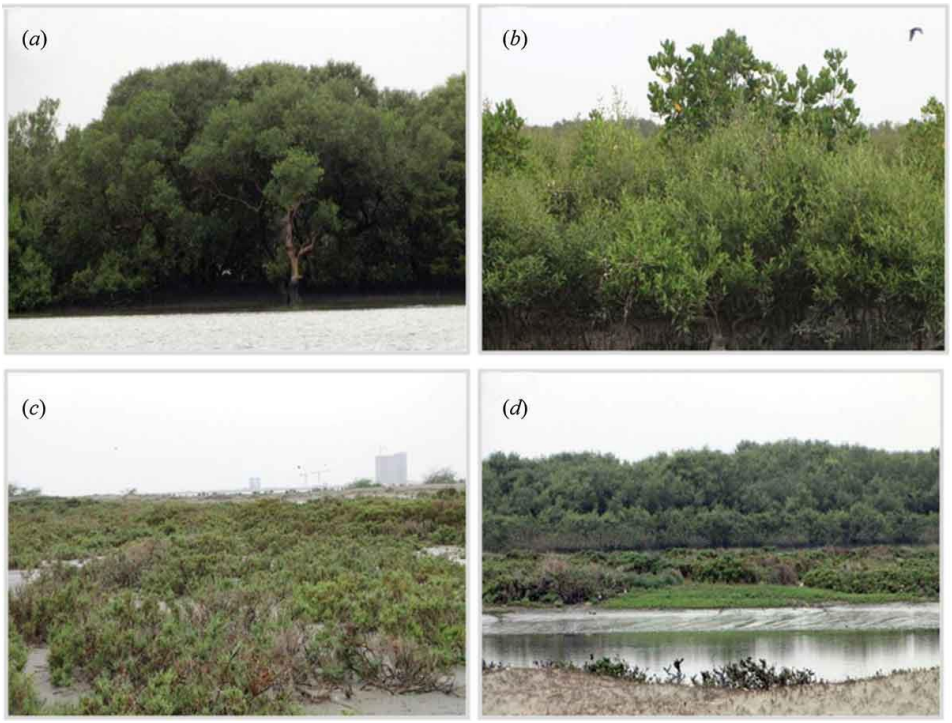

Figure 3. Field photographs (*a*) Close canopy (*Avicenna marina*) (*b*) Open canopy mangroves (*c*) Salt Bushes (*d*) Typifying example of diverse land cover features in the area

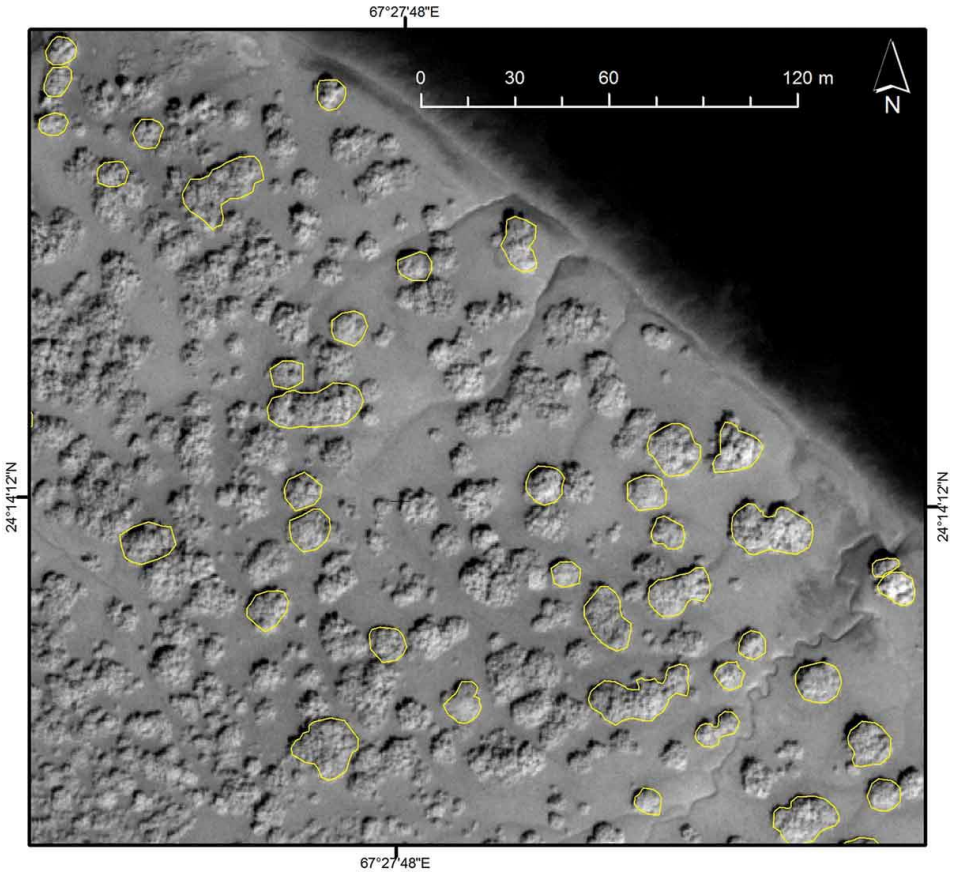

Figure 4. Reference polygons digitized on panchromatic image

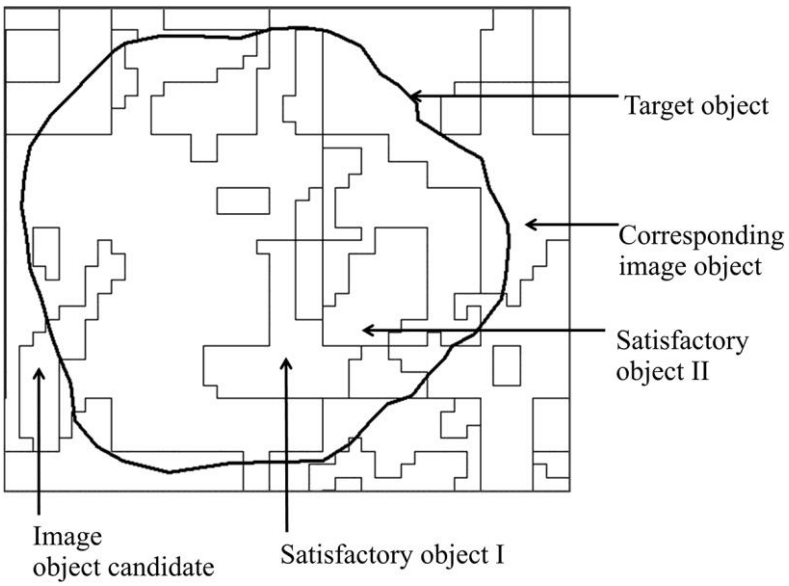

Figure 5. General classification schema of image segment for over and under segmentation

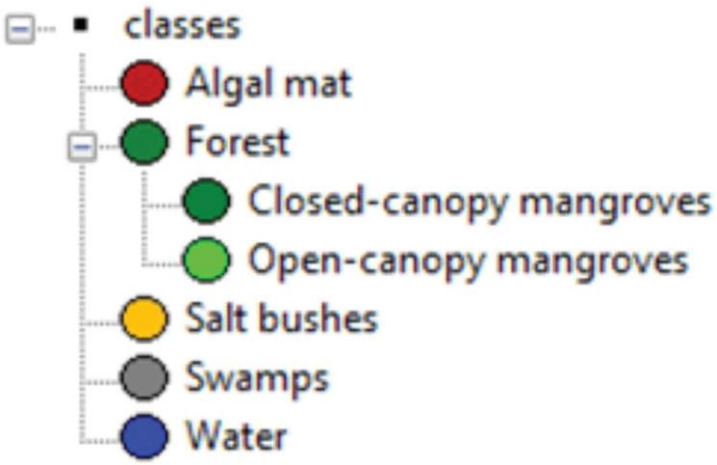

Figure 6. Class hierarchy

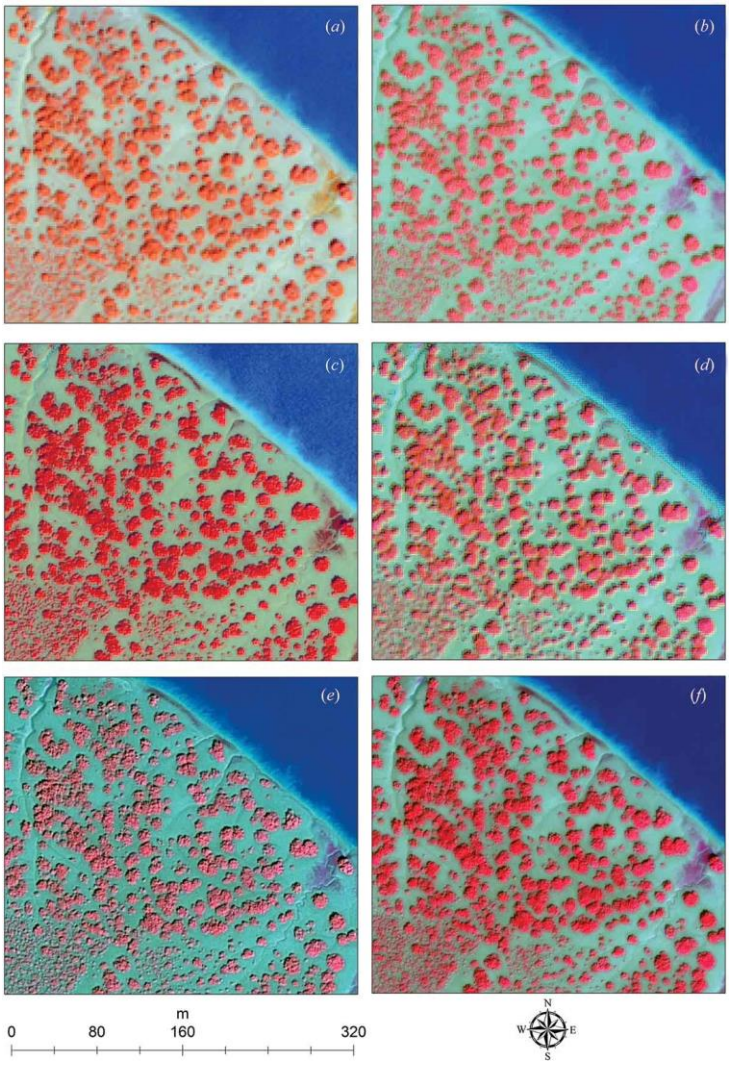

Figure 7. A representative sub scene of the original and fused images; (*a*) Original LRMI with RGB as 752; (*b*) HRMI by Ehler's fusion; (*c*) fused HRMI by modified IHS; (*d*) Wavelet transformation (*e*) fused image from optimized high pass filter addition; and (*f*) fused image of subtractive resolution merge

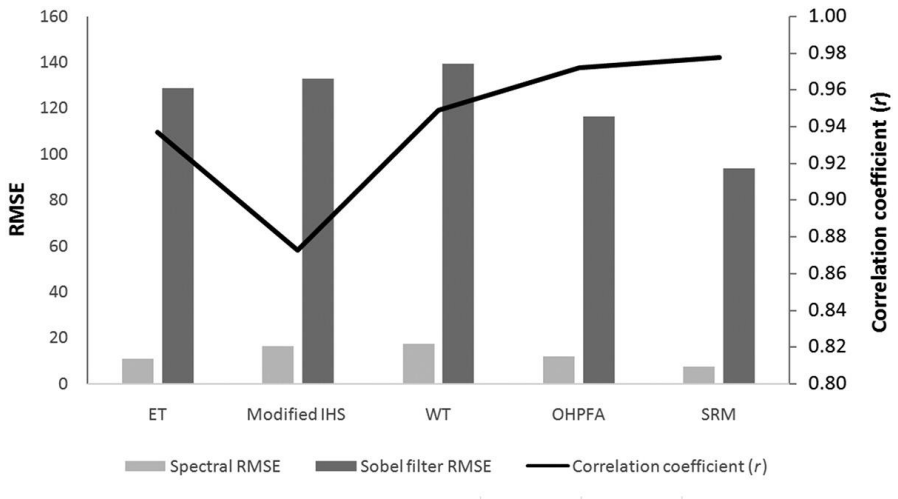

Figure 8. Average correlation and RMSE metrics for different techniques

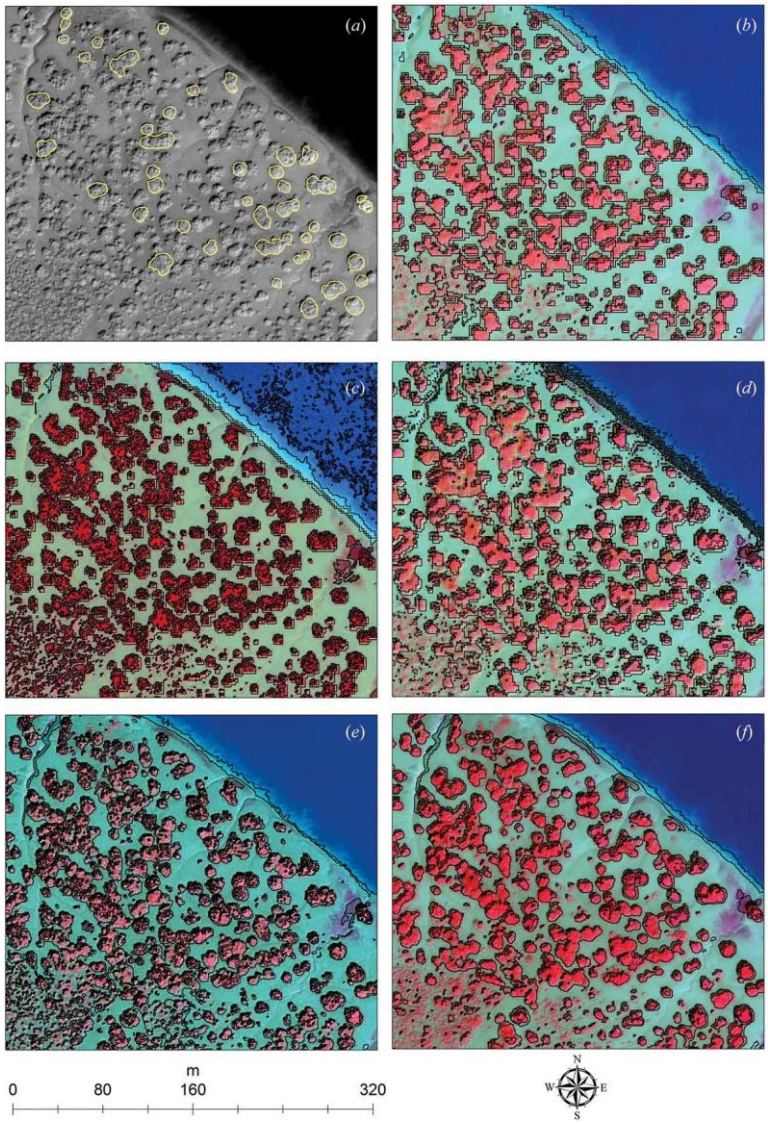

Figure 9. A comparison of (*a*) delineated crown canopies with segmented out of (*b*) ehler's transformation (*c*) modified IHS (*d*) wavelet transformation (*e*) optimized high pass filter addition (*f*) subtractive resolution merge

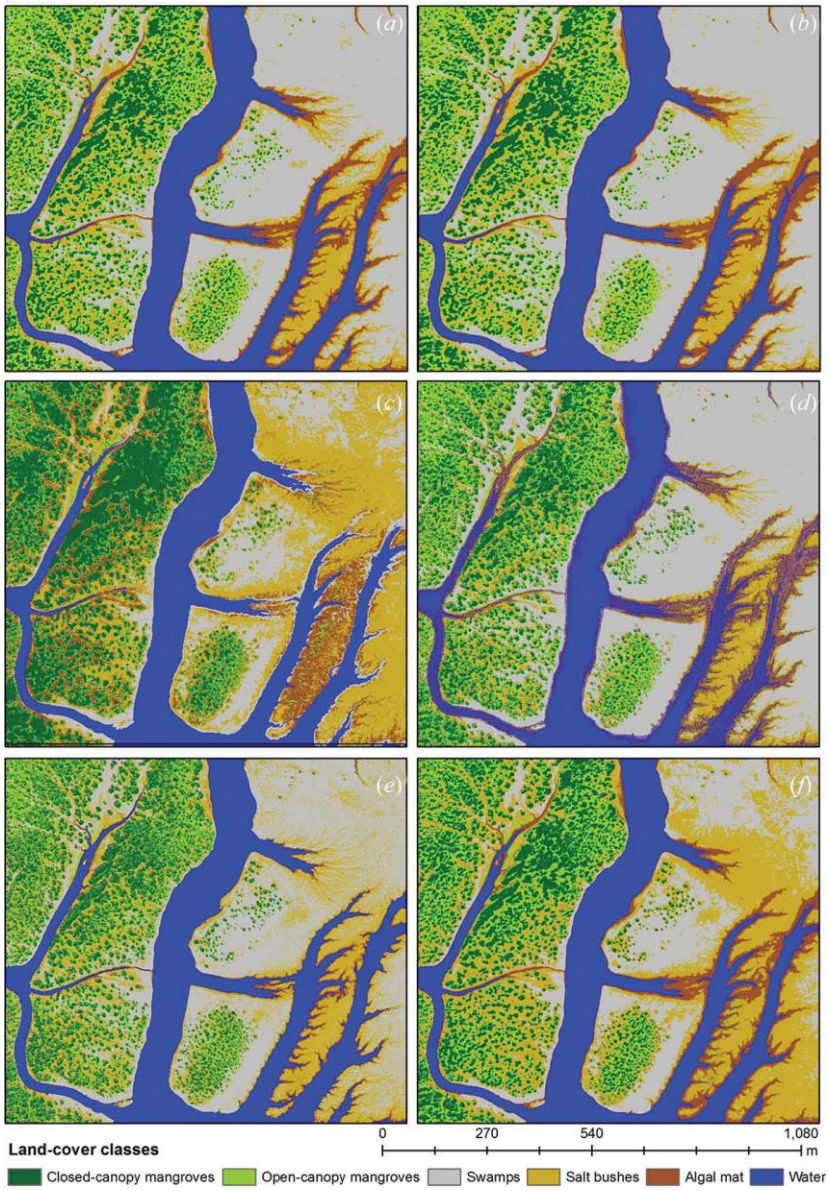

Figure 10. LC classes distribution generated from; (*a*) Original LRMI; (*b*) ET; (*c*) Modified IHS; (*d*) WT; (*e*) OHPFA; (*f*) SRM